Transit Met Chem (2017) 42:273–283
DOI 10.1007/s11243-016-0081-0

Synthesis, crystal structures, and properties of three coordination polymers of 5-(1H-imidazol-1-yl) isophthalic acid

Dong-Lin Fang[1] · Shao-Yin Mo[1] · Kai-Fei Wu[1] · Zhong-Jing Huang[1]

Received: 24 May 2016 / Accepted: 5 July 2016 / Published online: 8 March 2017

Abstract Three coordination polymers have been obtained by hydrothermal synthesis, namely $[Zn(imip)(H_2O)_2]\cdot 0.5H_2O$ (**1**), $[Co(imip)(H_2O)_2]\cdot 0.5H_2O$ (**2**), and $[Cd_2(imip)_2(H_2O)_3]$ (**3**) [H_2imip = 5-(1H-imidazol-1-yl) isophthalic acid]. The coordination polymers were characterized by IR spectra, elemental analysis, powder X-ray diffraction, and thermogravimetric analysis. Furthermore, single-crystal X-ray analysis reveals that they have 2D structures, which are extended into 3D networks via O–H···O hydrogen-bonding interactions. The luminescent properties of these coordination polymers were investigated.

Introduction

The design and synthesis of coordination polymers (CPs) has been an important area of research in recent decades [1–9]. These materials not only form intriguing architectures and topologies, but also find potential applications in the areas of luminescence, gas adsorption, catalysis, magnetic materials, drug delivery, and so on [10–21]. However, the prediction of final structures of such crystalline products is still a big challenge, since there are many factors that influence the self-assembly process, such as choice of organic ligands, metal ions, temperature, solvent system, and pH of the reaction system [22, 23]. Hydrothermal synthesis was proved to be an efficient strategy to provide a stable reaction environment [24, 25]. Some transition metals (Zn, Co, Cd) can be effectively chelated or bridged with carboxylic acid ligands [26]; hence, it is very important to choose appropriate metal ions and suitable organic nitrogen-donor or oxygen-donor ligands in the preparation of such materials [27].

Multi-carboxylate ligands have often been selected as multi-functional organic linkers, because of their variable coordination modes, which allow them to adopt various structural topologies [28]. 5-(1H-imidazol-1-yl) isophthalic acid, (H_2imip) which has two carboxylate and one nitrogen donors, has captured the attention of chemists of late [29]. Its coordination polymers have a wide range of structural diversities and potential applications as porous and magnetic materials; furthermore, multi-carboxylate ligands are also capable of functioning as hydrogen bond donors and/or acceptors [30].

In this work, H_2imip was chosen as a ligand for the preparation of functional coordination polymers with the transition metals Zn(II), Co(II), and Cd(II). This led to the successful synthesis of three new CPs, namely $[Zn(imip)(H_2O)_2]\cdot 0.5H_2O$ (**1**), $[Co(imip)(H_2O)_2]\cdot 0.5H_2O$ (**2**), and $[Cd_2(imip)_2(H_2O)_3]$ (**3**). All three CPs have been characterized by their IR spectra, elemental analysis, PXRD, and single-crystal X-ray crystallography. In addition, the solid-state photoluminescent properties at room temperature and the thermal decomposition processes of the complexes were investigated.

Experimental

All starting materials were purchased commercially and used without further purification. These included H_2imip (Xiya, 99 %), $Zn(OAc)_2\cdot 2H_2O$, $CoSO_4\cdot 7H_2O$, $Cd(NO_3)_2\cdot 4H_2O$ (Aladdin, 99 %), and NaOH (Kelon, 99 %). Elemental analyses for C, H, and N were obtained on a PerkinElmer

---

✉ Zhong-Jing Huang
zhongjinghuang@163.com

[1] College of Chemistry and Chemical Engineering, Guangxi University for Nationalities, Nanning 530006, People's Republic of China

Table 1 Crystallographic data for polymers **1**–**3**

Polymer	**1**	**2**	**3**
Formula	$C_{22}H_{22}N_4O_{13}Zn_2$	$C_{22}H_{20}Co_2N_4O_{13}$	$C_{22}H_{18}Cd_2N_4O_{11}$
Formula weight	681.18	668.28	739.20
Crystal system	Monoclinic	Monoclinic	Triclinic
Space group	*P2(1)/c*	*P2(1)/c*	*P-1*
a (Å)	10.743(14)	10.771(7)	6.8646(2)
b (Å)	16.77(2)	16.880(11)	10.8997(4)
c (Å)	7.336(9)	7.391(5)	17.2065(6)
α (°)	90	90	90.1310(10)
β (°)	95.402(17)	97.046(14)	96.9130(10)
γ (°)	90	90	104.7640(10)
Volume (Å^3)	1316(3)	1333.6(16)	1235.14(7)
$D_{calc.}$ (Mg m^{-3})	1.719	1.659	1.988
Z	2	2	2
Absorption coefficient (mm^{-1})	1.898	1.659	1.791
F(000)	692	676	724
Crystal size (mm^3)	0.23 × 0.22 × 0.21	0.13 × 0.12 × 0.11	0.18 × 0.17 × 0.16
θ range (°)	1.90–25.00	1.90–25.00	1.19–25.26
Reflections collected	6627	7081	4454
Unique reflections	2299 [R(int) = 0.0568]	2322 [R(int) = 0.0550]	4454 [R(int) = 0.0000]
Completeness to $\vartheta = 25.00$	99.1 %	98.5 %	99.3 %
Max. and min. transmission	0.6913 and 0.6693	0.8686 and 0.8474	0.763 and 0.739
Data/restraints/parameters	2299/6/190	2320/6/190	4454/0/352
GOF on F^2	1.081	1.064	1.065
R indices [$I > 2\sigma(I)$]	R1 = 0.1003, wR2 = 0.2581	R1 = 0.0846, wR2 = 0.2260	R1 = 0.0229, wR2 = 0.0600
R indices (all data)	R1 = 0.1123, wR2 = 0.2662	R1 = 0.0927, wR2 = 0.2320	R1 = 0.0246, wR2 = 0.0608
Largest diff. peak and hole (e Å^{-3})	2.530 and −1.012	2.003 and −0.649	1.139 and −0.505

2400 II elemental analyzer. FTIR spectra were obtained on a PE Spectrum One FTIR spectrometer in the 4000–400 cm^{-1} region, using KBr pellets. A PerkinElmer Diamond TG/DTA thermal analyzer was used to record simultaneous TG and DTG curves in a static air atmosphere at a heating rate of 10 K min^{-1} in the temperature range of 25–1000 °C using platinum crucibles. Fluorescence spectra were recorded on an F-4600 FL spectrophotometer analyzer. Powder X-ray diffraction patterns were obtained using a pinhole camera (Anton Paar) operating with point-focused Ni-filtered Cu Kα radiation in the 2θ range from 10° to 50° at a scan rate of 0.08° per second.

Synthesis of complex 1

A mixture of $Zn(OAc)_2 \cdot 2H_2O$ (43.9 mg, 0.2 mmol), H_2imip (46.4 mg, 0.2 mmol), NaOH (16 mg, 0.4 mmol), and water (9 mL) was sealed in a Teflon-lined stainless steel autoclave reactor (25 mL) and heated at 140 °C for 3 days. After cooling to room temperature at a rate of 5 °C h^{-1}, colorless block crystals of complex **1** were obtained in a yield of 56 % based on H_2imip. Calcd. for $C_{22}H_{22}N_4O_{13}Zn_2$: C, 38.75; H, 3.23; N, 8.22; Found: C, 38.81; H, 3.28; N, 8.27; IR (KBr, cm^{-1}): 3420(s), 3143(m), 1634(s), 1582(s), 1558(m), 1541(m), 1509(m), 1456(m), 1433(m), 1385(s), 1317(m), 1265(m), 1072(s), 776(s), 744(s), 722(s).

Synthesis of complex 2

Complex **2** was prepared by a similar procedure to that for complex **1**, by using a mixture of $CoSO_4 \cdot 7H_2O$ (56.2 mg, 0.2 mmol), H_2imip (46.4 mg, 0.2 mmol), and NaOH (16 mg, 0.4 mmol). Red block crystals were obtained in 70 % yield based on H_2imip. Calcd. for $C_{22}H_{20}Co_2N_4O_{13}$: C, 39.50; H, 3.29; N, 8.38; Found: C, 39.57; H, 3.23; N, 8.42; IR (KBr, cm^{-1}): 3446(s), 3137(m), 1626(s), 1579(s), 1508(s), 1434(s), 1393(s), 1316(m), 1265(m), 1072(s), 776(s), 744(s), 722(s).

Synthesis of complex 3

Complex **3** was prepared by a similar procedure to that used for complex **1**, using a mixture of $Cd(NO_3)_2 \cdot 4H_2O$ (61.7 mg, 0.2 mmol), H_2imip (46.4 mg, 0.2 mmol), and NaOH

Table 2 Selected bond lengths (Å) and angles (°) for **1–3**

1			
Zn(1)–O(3)	2.027(7)	Zn(1)–N(2)#1	2.036(7)
Zn(1)–O(2)	2.051(6)	Zn(1)–O(1)	2.075(6)
Zn(1)–O(5)#2	2.147(7)	Zn(1)–O(6)#2	2.461(8)
O(5)–Zn(1)#3	2.147(7)	O(6)–Zn(1)#3	2.461(8)
N(2)–Zn(1)#4	2.036(7)	O(3)–Zn(1)–N(2)#1	96.6(3)
O(3)–Zn(1)–O(2)	88.8(3)	N(2)#1–Zn(1)–O(2)	94.9(3)
O(3)–Zn(1)–O(1)	88.7(3)	N(2)#1–Zn(1)–O(1)	96.4(3)
O(2)–Zn(1)–O(1)	168.7(2)	O(3)–Zn(1)–O(5)#2	166.9(3)
N(2)#1–Zn(1)–O(5)#2	96.5(3)	O(2)–Zn(1)–O(5)#2	89.3(3)
O(1)–Zn(1)–O(5)#2	90.7(3)	O(3)–Zn(1)–O(6)#2	110.7(3)
N(2)#1–Zn(1)–O(6)#2	152.7(3)	O(2)–Zn(1)–O(6)#2	85.8(2)
O(1)–Zn(1)–O(6)#2	84.8(2)	O(5)#2–Zn(1)–O(6)#2	56.3(3)
C(1)–O(3)–Zn(1)	132.6(6)	C(5)–O(5)–Zn(1)#3	98.4(6)
C(5)–O(6)–Zn(1)#3	84.0(5)	C(9)–N(2)–Zn(1)#4	126.1(6)
C(10)–N(2)–Zn(1)#4	127.7(6)		
2			
Co(1)–O(3)	2.077(5)	Co(1)–N(2)	2.093(5)
Co(1)–O(2)	2.098(6)	Co(1)–O(1)	2.098(6)
Co(1)–O(5)	2.159(5)	Co(1)–O(6)	2.341(5)
O(3)–Co(1)–N(2)	92.4(2)	O(3)–Co(1)–O(2)	88.2(2)
N(2)–Co(1)–O(2)	95.8(2)	O(3)–Co(1)–O(1)	88.3(2)
N(2)–Co(1)–O(1)	94.6(2)	O(2)–Co(1)–O(1)	169(2)
O(3)–Co(1)–O(5)	171.7(2)	N(2)–Co(1)–O(5)	95.8(2)
O(2)–Co(1)–O(5)	92.3(2)	O(1)–Co(1)–O(5)	89.7(2)
O(3)–Co(1)–O(6)	113.48(19)	N(2)–Co(1)–O(6)	154.10(19)
O(2)–Co(1)–O(6)	85.62(19)	O(1)–Co(1)–O(6)	86.46(19)
O(5)–Co(1)–O(6)	58.33(18)	C(1)–O(3)–Co(1)	131.7(4)
C(8)–O(5)–Co(1)	94.9(4)	C(8)–O(6)–Co(1)	86.5(4)
3			
Cd(1)–O(9)#1	2.178(2)	Cd(1)–N(3)	2.222(2)
Cd(1)–O(6)	2.333(2)	Cd(1)–O(7)	2.350(2)
Cd(1)–O(5)	2.420(2)	Cd(1)–O(6)#2	2.504(2)
Cd(2)–O(4)	2.199(2)	Cd(2)–N(1)#1	2.267(2)
Cd(2)–O(2)	2.328(3)	Cd(2)–O(10)#3	2.343(2)
Cd(2)–O(1)	2.349(3)	Cd(2)–O(11)#3	2.451(2)
Cd(2)–C(21)#3	2.743(3)	O(6)–Cd(1)#2	2.504(2)
O(9)–Cd(1)#4	2.178(2)	O(10)–Cd(2)#5	2.343(2)
O(11)–Cd(2)#5	2.451(2)	N(1)–Cd(2)#4	2.267(2)
C(21)–Cd(2)#5	2.743(3)	O(9)#1–Cd(1)–N(3)	92.68(9)
O(9)#1–Cd(1)–O(6)	127.25(8)	N(3)–Cd(1)–O(6)	138.64(8)
O(9)#1–Cd(1)–O(7)	85.20(8)	N(3)–Cd(1)–O(7)	102.49(9)
O(6)–Cd(1)–O(7)	92.33(8)	O(9)#1–Cd(1)–O(5)	167.03(9)
N(3)–Cd(1)–O(5)	88.54(8)	O(6)–Cd(1)–O(5)	55.27(7)
O(7)–Cd(1)–O(5)	81.93(8)	O(9)#1–Cd(1)–O(6)#2	88.90(8)
N(3)–Cd(1)–O(6)#2	94.16(8)	O(6)–Cd(1)–O(6)#2	78.23(7)
O(7)–Cd(1)–O(6)#2	162.56(8)	O(5)–Cd(1)–O(6)#2	103.90(7)
O(4)–Cd(2)–N(1)#1	87.52(9)	O(4)–Cd(2)–O(2)	91.04(11)
N(1)#1–Cd(2)–O(2)	100.27(9)	O(4)–Cd(2)–O(10)#3	129.88(8)
N(1)#1–Cd(2)–O(10)#3	142.46(8)	O(2)–Cd(2)–O(10)#3	84.22(9)
O(4)–Cd(2)–O(1)	90.37(11)	N(1)#1–Cd(2)–O(1)	97.76(9)

Table 2 continued

O(2)–Cd(2)–O(1)	161.97(10)	O(10)#3–Cd(2)–O(1)	81.10(9)
O(4)–Cd(2)–O(11)#3	175.72(8)	N(1)#1–Cd(2)–O(11)#3	88.23(8)
O(2)–Cd(2)–O(11)#3	89.18(9)	O(10)#3–Cd(2)–O(11)#3	54.39(7)
O(1)–Cd(2)–O(11)#3	90.74(10)	O(4)–Cd(2)–C(21)#3	157.09(9)
N(1)#1–Cd(2)–C(21)#3	115.35(8)	O(2)–Cd(2)–C(21)#3	86.36(10)
O(10)#3–Cd(2)–C(21)#3	27.21(8)	O(1)–Cd(2)–C(21)#3	85.36(9)
O(11)#3–Cd(2)–C(21)#3	27.19(8)	C(10)–O(4)–Cd(2)	115.7(2)
C(11)–O(5)–Cd(1)	90.01(16)	C(11)–O(6)–Cd(1)	92.83(16)
C(11)–O(6)–Cd(1)#2	118.43(17)	Cd(1)–O(6)–Cd(1)#2	101.76(7)
C(22)–O(9)–Cd(1)#4	121.7(2)	C(21)–O(10)–Cd(2)#5	94.44(17)
C(21)–O(11)–Cd(2)#5	89.53(17)	C(3)–N(1)–Cd(2)#4	130.59(19)
C(1)–N(1)–Cd(2)#4	123.38(18)	C(14)–N(3)–Cd(1)	128.7(2)
C(12)–N(3)–Cd(1)	123.28(19)	O(11)–C(21)–Cd(2)#5	63.28(15)
O(10)–C(21)–Cd(2)#5	58.36(14)	C(19)–C(21)–Cd(2)#5	176.92(19)

Symmetry transformations used to generate equivalent atoms: for Polymer **1**: #1 x + 1, y, z #2 −x + 1, y + 1/2, −z + 3/2 #3 −x + 1, y−1/2, −z + 3/2 #4 x−1, y, z; for Polymer **2**: #1 −x + 1, y−1/2, −z + 3/2 #2 −x + 2, y + 1/2,−z + 3/2 #3 −x + 2, y−1/2, −z + 3/2 #4 −x + 1, y + 1/2,−z + 3/2; and for Polymer **3**: #1 x, y + 1, z #2 −x + 2, −y + 1, −z + 1 #3 x, y + 1, z + 1 #4 x, y−1, z #5 x, y−1, z−1

Table 3 Hydrogen bond geometry (Å) for polymers **1**–**3**

D–H···A	D–H	H···A	D···A	D–H···A
Polymer **1**				
O(7)–H(7D)···O(7)#5	0.85	1.68	2.51(5)	164.2
O(7)–H(7C)···O(4)#2	0.85	2.10	2.93(2)	165.2
O(2)–H(2D)···O(6)#6	0.85	2.02	2.822(10)	158.1
O(2)–H(2C)···O(4)#7	0.85	2.02	2.827(10)	158.2
O(1)–H(1D)···O(6)#8	0.85	2.01	2.813(10)	158.0
O(1)–H(1C)···O(4)#9	0.85	2.03	2.840(10)	158.2
Polymer **2**				
O(2)–H(2D)···O(6)#5	0.85	2.03	2.846(7)	159.5
O(2)–H(2C)···O(4)#5	0.85	1.97	2.782(8)	159.1
O(1)–H(1D)···O(6)#6	0.85	2.00	2.813(8)	159.7
O(1)–H(1C)···O(4)#6	0.85	1.96	2.769(8)	159.9
Polymer **3**				
O(1)–H(1D)···O(3)#6	0.85	1.89	2.652(4)	148.9
O(1)–H(1A)···O(4)	0.85	2.53	3.228(4)	140.0
O(2)–H(2C)···O(1)#7	0.85	2.12	2.975(4)	179.7
O(2)–H(2C)···O(3)#8	0.85	2.58	3.001(4)	111.9
O(2)–H(2D)···O(10)#9	0.85	1.87	2.721(3)	179.1
O(7)–H(7C)···O(6)#10	0.85	2.15	2.973(3)	163.2
O(7)–H(7D)···O(8)#9	0.85	1.91	2.737(3)	162.7

(16 mg, 0.4 mmol). Colorless block crystals were obtained in 68 % yield based on H_2imip. Calcd. for $C_{22}H_{18}Cd_2N_4O_{11}$: C, 35.71; H, 2.44; N, 7.57; Found: C, 35.76; H, 2.48; N, 7.62; IR (KBr, cm^{-1}): 3448(s), 3150(m), 1626(s), 1584(s), 1548(s), 1464(s), 1401(s), 1120(m), 1067(s), 774(s), 744(s), 670(s).

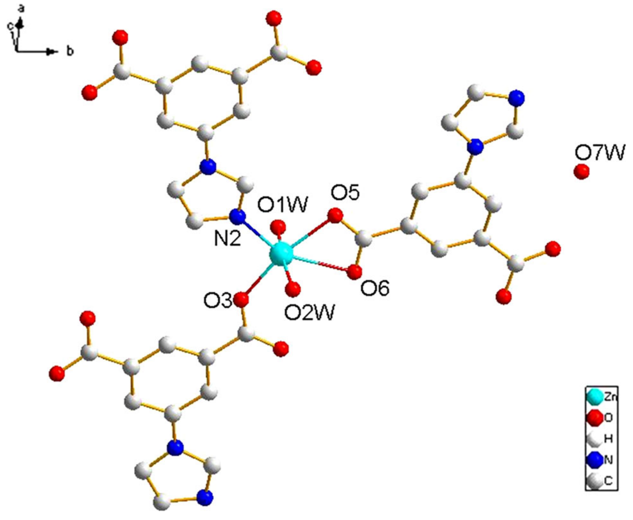

Fig. 1 Coordination environment of Zn in complex **1**. All the hydrogen atoms are omitted for clarity

Crystal structure determination

Suitable single crystals with approximate dimensions (0.11 × 0.11 × 0.11 mm^3) were mounted on a glass fiber and used for X-ray diffraction analyses. The data were collected on a Bruker SMART CCD diffractometer at 293(2) K, using graphite-monochromatized Mo Kα radiation ($\lambda = 0.71069$ Å). Absorption corrections were applied using SADABS. All structures were solved by direct methods and refined by full-matrix least squares on F2

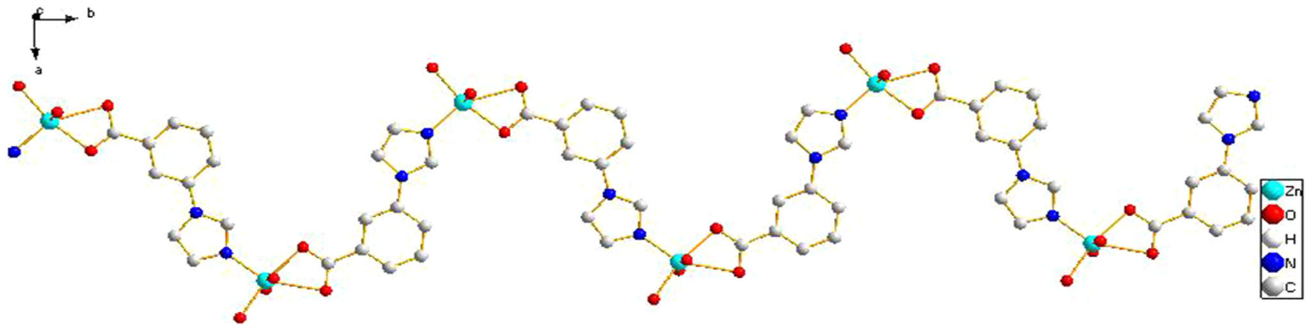

Fig. 2 An interesting infinitely extended S curve chain of complex **1**. Unnecessary atoms are omitted for clarity

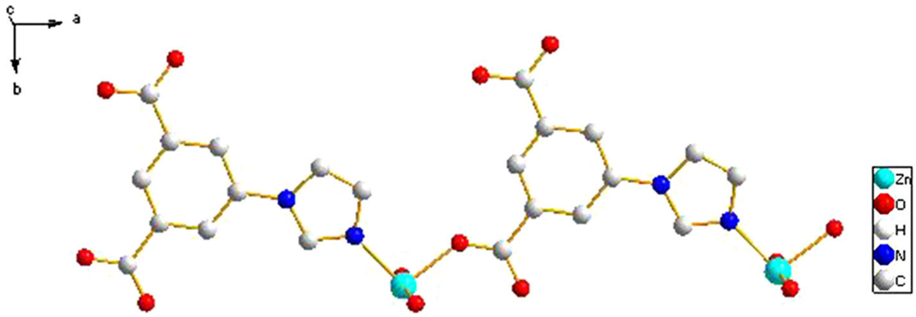

Fig. 3 One-dimensional linear chain of complex **1** along a axis. Unnecessary atoms are omitted for clarity

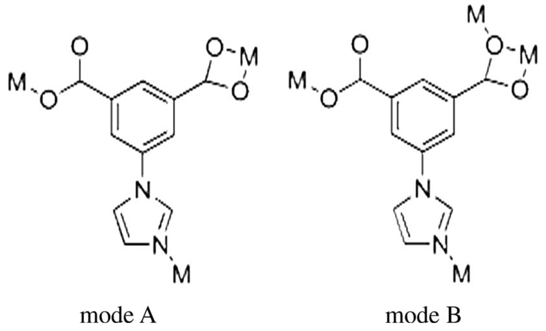

Scheme 1 Coordination Modes of the carboxylate group in H_2imip

using the SHELXTL-97 program package [31]. All non-hydrogen atoms were refined with anisotropic displacement parameters. Hydrogen atoms attached to carbon were placed in geometrically idealized position and refined using a riding model. The crystallographic data as well as details of the data collection and refinement are listed in Table 1. Selected bond lengths and angles are given in Table 2, and hydrogen bond geometries are given in Table 3.

Results and discussion

Description of the structures

Single-crystal X-ray diffraction analysis reveals that in spite of their different metal centers, complexes **1** and **2** are isostructural; hence, only the structure of complex **1** is discussed here. Complex **1** crystallizes in the monoclinic system, space group *P2(1)/c*. As shown in Fig. 1, the Zn atom has a six-coordinate mode, provided by three oxygen atoms from different imip ligands plus a further two oxygen atoms from two coordinated water ligands. The remaining coordination site is occupied by a nitrogen atom from the third imip ligand. The relevant bond lengths are Zn–O3 = 2.027(7) Å, Zn–O5 = 2.147(7) Å, Zn–O6 = 2.461(8) Å, Zn–O1(W) = 2.075(6) Å, Zn–O2(W) = 2.051(6) Å, and Zn–N2 = 2.036(7) Å. The O1W–Zn–N2, O1W–Zn–O3, O1W–Zn–O2W, and O1W–Zn–O5 bond angles are 96.4(3)°, 88.7(3)°, 168.7(2)°, and 90.7(3)°, respectively. The two water ligands occupy the axial positions, in a slightly distorted octahedral geometry overall. In complex **2**, the relevant bond lengths are Co–O3 = 2.077(5) Å, Co–O5 = 2.159(5) Å, Co–O6 = 2.341(5) Å, Co–O1(W) = 2.098(6) Å, and Co–O2(W) = 2.098(6) Å, while the O1W–Co–N2, O1W–Co–O3, O1W–Co–O2W, and O1W–Co–O5 band angles are 94.6(2)°, 88.3(2)°, 169(2)°, and 89.7(2)°, respectively (Figs. 2, 3).

In complexes **1** and **2**, the carboxylate groups of the imip^{2-} ligands adopt two different coordination modes (mode A, scheme 1) to connect the metal atoms. As shown in Fig. 4, it is apparent that the organic anions play an important role in determining the structures of these metal–organic complexes. Furthermore, each imip ligand joins three metal centers together and each metal center is coordinated by three imip ligands, resulting in infinite two-dimensional network structures. There are several

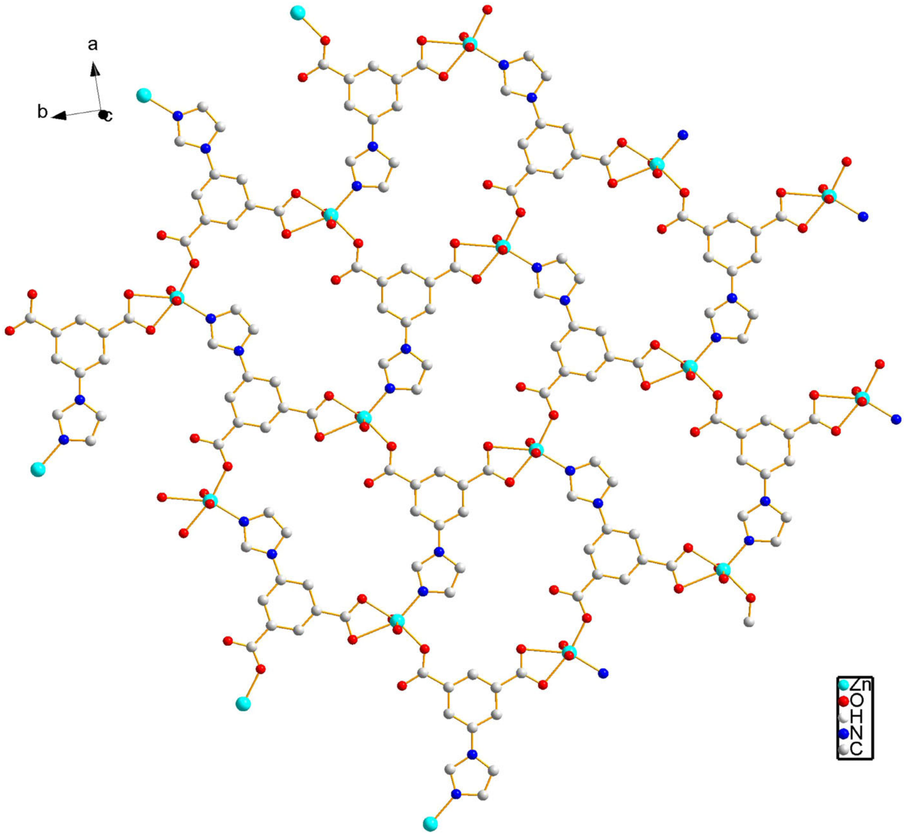

Fig. 4 Two-dimensional network structures of complex **1** in the *ab* plane. Unnecessary atoms are omitted for clarity

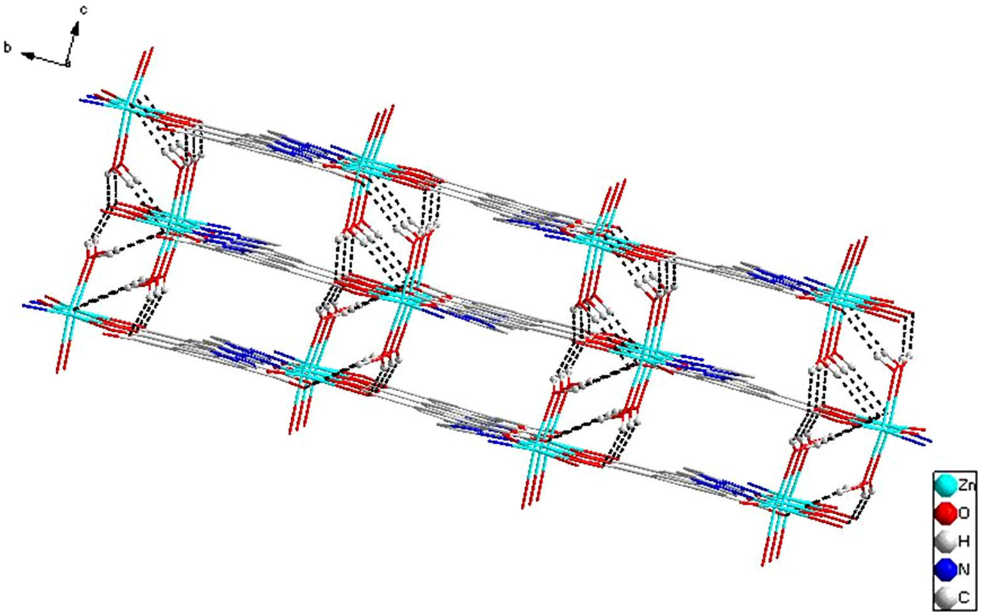

Fig. 5 Three-dimensional polymeric frameworks of complex **1** connected by O–H···O hydrogen bonds (*black dashed line*). Unnecessary atoms are omitted for clarity

different hydrogen bonds, namely O(2)–H(2D)···O(6)#6, O(2)–H(2C)···O(4)#7, O(1)-H(1D)···O(6)#8, and O(1)–H(1C)···O(4)#9. The O···O distances all fall in the range of 2.51(5)–2.93(2) Å. The 2D structure is extended into a 3D framework via O–H···O hydrogen-bonding interactions (Fig. 5).

Complex **3** crystallizes in the triclinic system, space group *P-1*. There are two Cd atoms, two imip ligands, and three water molecules in the asymmetric unit. As shown in Fig. 6, in coordination polymer **3**, the two symmetrically independent cadmium atoms adopt distinct coordination environments. The Cd1 atom has a six-coordinate mode

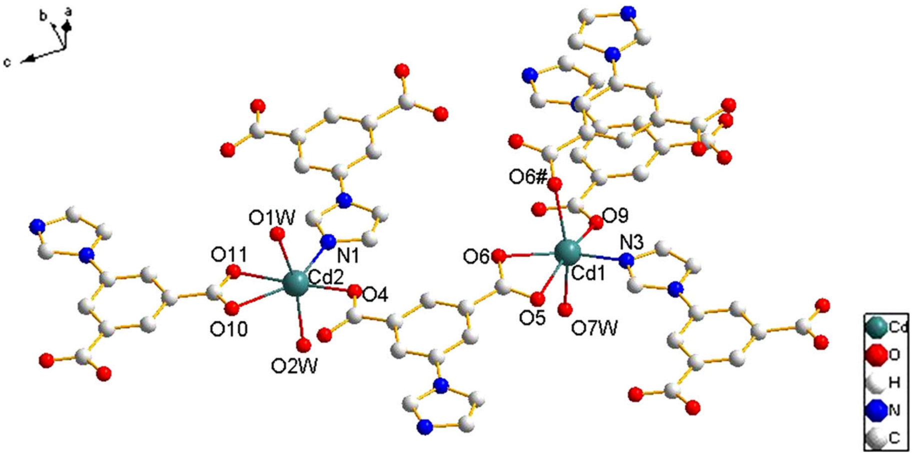

Fig. 6 Coordination environment of Cd in complex **3**. All the hydrogen atoms are omitted for clarity

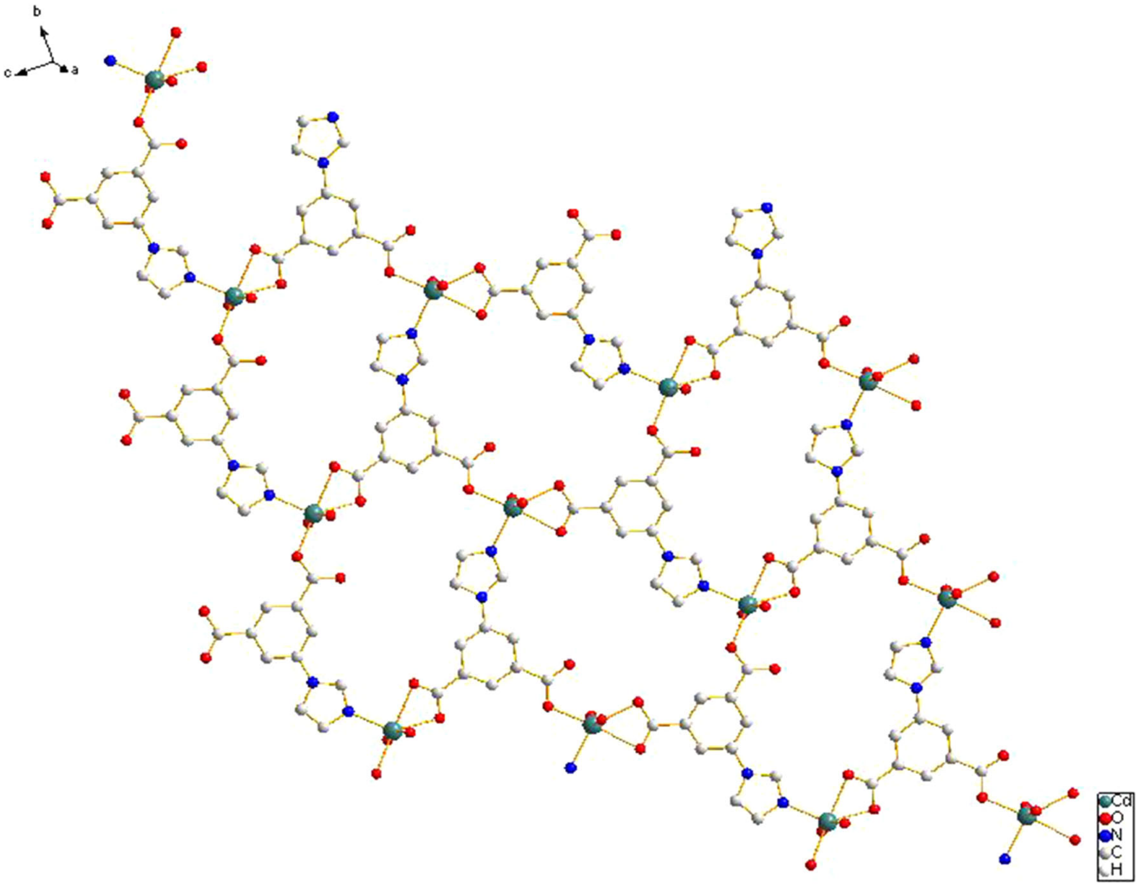

Fig. 7 Two-dimensional network structures of complex **3** in the bc plane. All the hydrogen atoms are omitted for clarity

with four oxygen atoms from three different imip ligands and a further oxygen atom from a coordinated water ligand, while the remaining coordination site is occupied by a nitrogen atom from the fourth imip ligand. The Cd2 atom has a six-coordinate mode, provided by three oxygen atoms from two different imip ligands and two more oxygen atoms from two coordinated water ligands; the final coordination site is occupied by a nitrogen atom from the third imip ligand. Unlike complexes **1**–**2**, the imip^{2-} ligand in **3** adopts a novel coordination mode (mode B, Scheme 1). In mode B, the imip acts as a imidazole ligand to coordinate with four cadmium ions. As shown in Fig. 7, the three carboxylic oxygen atoms in bidentate and monodentate coordination modes, plus one nitrogen atom of each imip ligand, link the metal centers to form an interesting infinitely extended 2D network structure. In addition, we

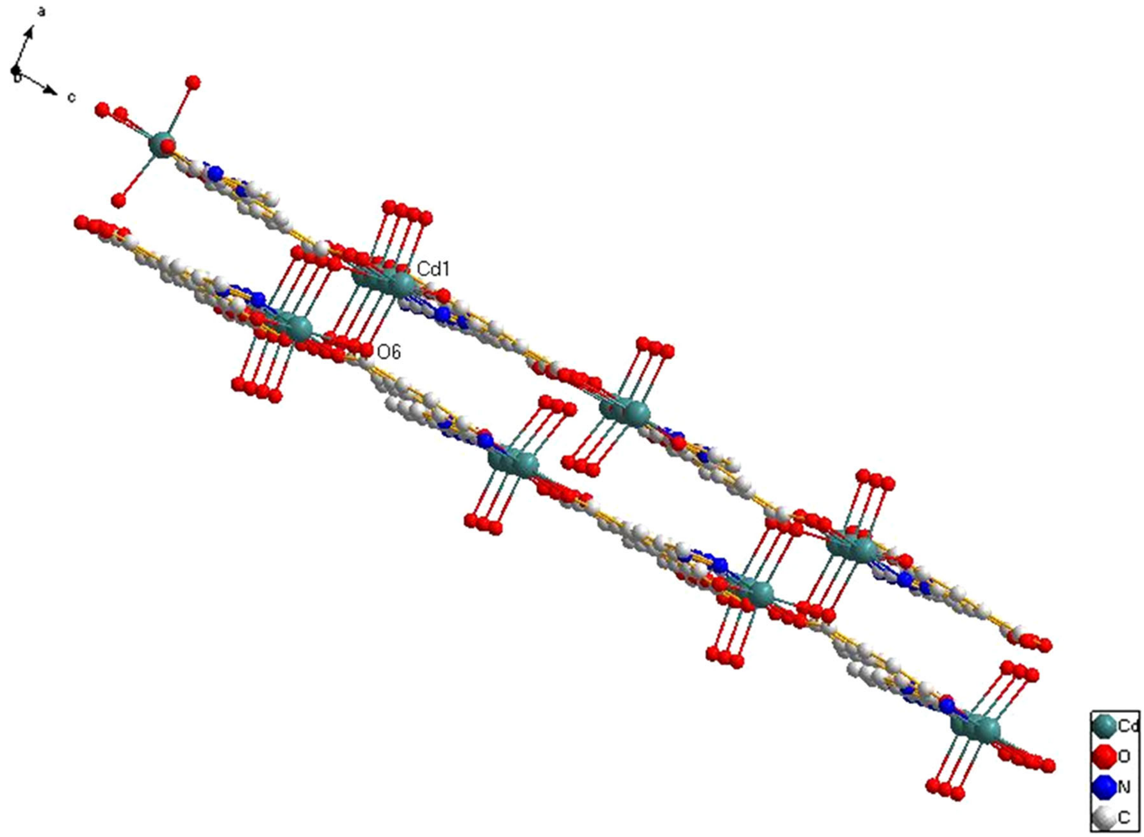

Fig. 8 Two neighboring planes of complex **3** connect by Cd1-O6. All the hydrogen atoms are omitted for clarity

observe two neighboring planes connected by a group of carboxylate oxygen atoms in chelating-bridging tridentate coordination modes (Fig. 8). The hydrogen bond lengths are O(1)–H(1D)···O(3)#6 = 2.652(4) Å, O(1)–H(1A)···O(4) = 3.228(4) Å, O(2)–H(2C)···O(1)#7 = 2.975(4) Å, O(2)–H(2C)···O(1)#7 = 3.001(4) Å, O(2)–H(2D)···O(10)#9 = 2.721(3) Å, O(7)–H(7C)···O(6)#10 = 2.973(3) Å, and O(7)–H(7D)···O(8)#9 = 2.737(3) Å. Figure 7 shows the 3D polymeric frameworks formed by these OH···O hydrogen-bonding interactions.

Spectroscopic and XRD properties

In the IR spectra of all three complexes, strong and broad absorption bands at about 3420–3448 cm^{-1} are attributed to the water ligand symmetric O–H stretching and O–H bending modes, respectively. The medium intensity bands at 3150–3137 cm^{-1} are assigned to the stretching vibrations of the aromatic C–H groups, while the bands at about 1582, 1509, 1456, and 1385 cm^{-1} are assigned to the stretching vibrations of the aromatic C=C and C=N bonds. The COO^- of the coordinated carboxyl group takes give rise to asymmetric and symmetric stretches at 1630 and 1265 cm^{-1} in **1**, 1626 and 1265 cm^{-1} in **2**, and at 1626 and 1120 cm^{-1} in **3** (Fig. 9).

In view of the excellent luminescence properties of coordination polymers with d10 metal centers and their potential applications in chemical sensors and photochemistry displays, the luminescence properties of the free H_2imip ligand and complexes **1** and **3** were investigated in the solid state at room temperature. As shown in Fig. 10, an emission peak was observed at 359 nm for H_2imip ($\lambda_{ex} = 274$ nm), which can be ascribed to ligand-centered transitions [32]. Under the same excitation conditions, emission peaks were observed at 363 nm for complex **1** ($\lambda_{ex} = 268$ nm), and 365 nm for complex **3** ($\lambda_{ex} = 294$ nm). Thus, compared to H_2imip, the emission maxima of **1** and **3** are redshifted. The most likely emission mechanism is ligand-to-metal charge transfer (LMCT) [33], given the similar emission bands observed for the free ligand and its complexes. The enhanced luminescence in the complexes can be attributed to the ligand coordination to the metal center, which enhances its rigidity and thus reduces the loss of energy through radiationless pathways [34].

The observed and simulated powder XRD patterns of the complex are depicted in Fig. 11. The measured powder

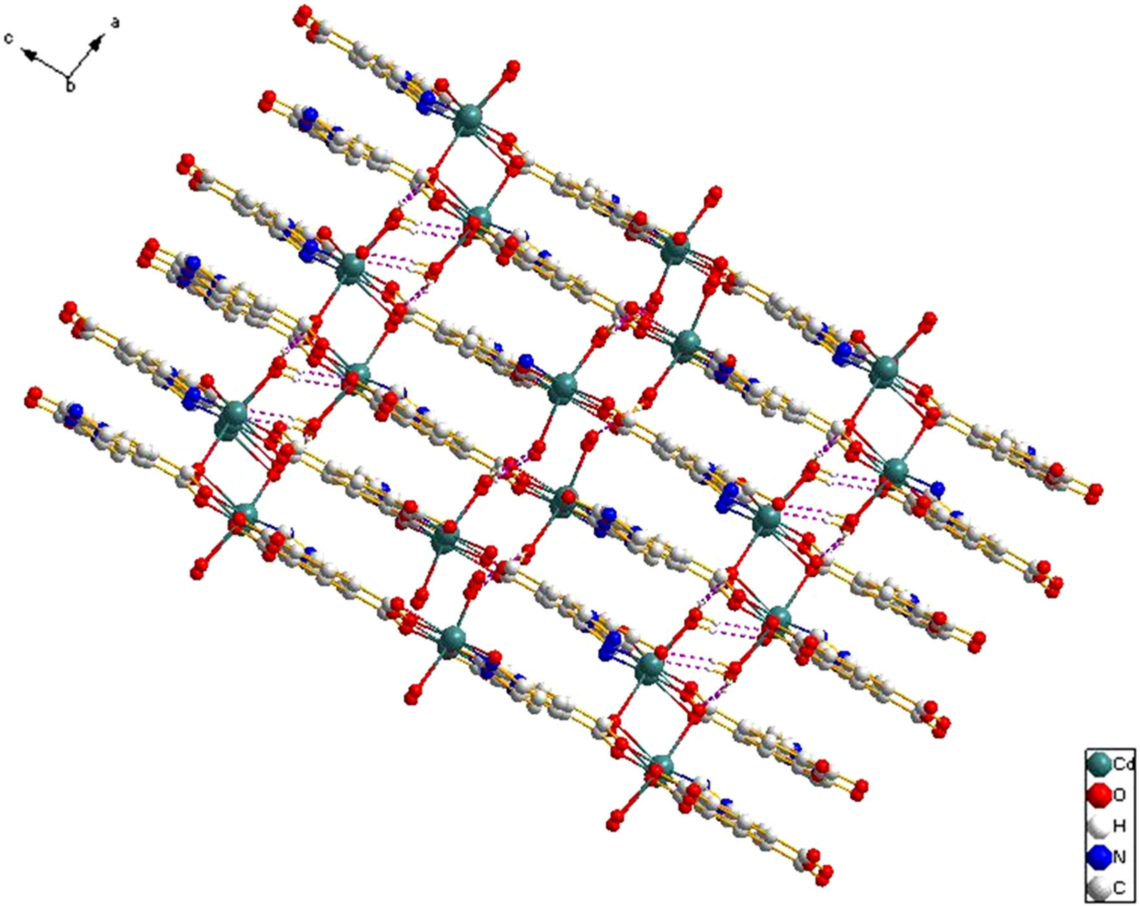

Fig. 9 Three-dimensional polymeric frameworks of complex **3** connected by O–H…O hydrogen bonds (*purple dashed line*). Unnecessary atoms are omitted for clarity. (Color figure online)

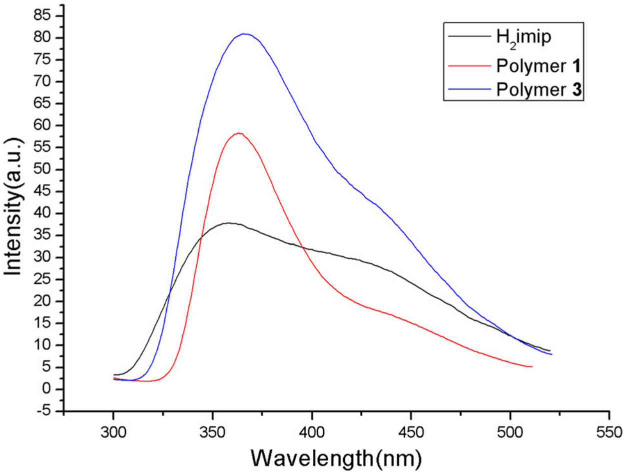

Fig. 10 Solid-state fluorescence emissions recorded at room temperature for free ligand and complexes **1** and **3**

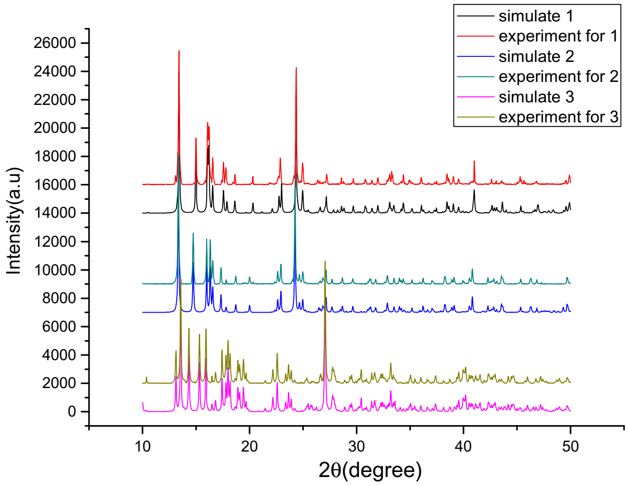

Fig. 11 XRD patterns of the complexes **1**–**3**

XRD patterns are in good agreement with the patterns simulated from the X-ray single-crystal data, confirming the phase purities of the samples. The differences in reflection intensities between the simulated and experimental patterns can be explained by the different orientations of the crystals in the bulk powder sample.

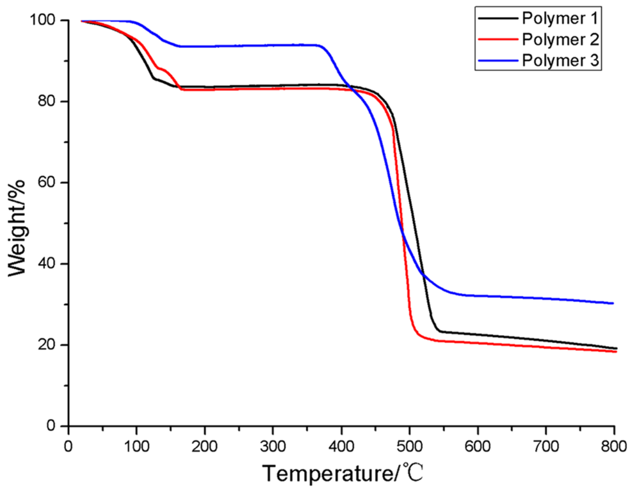

Fig. 12 TG curves for complexes **1**–**3**

Thermogravimetric analyses

Thermogravimetric (TG) analysis was performed in air on freshly grown air-dried crystals of the complexes, and the resulting TG curves are shown in Fig. 12. The first stage indicates that complexes **1** and **2** lose 16.2 and 17.1 % of their respective total weights at temperatures ranging from room temperature to 115 °C for **1** and 131 °C for **2**. These weight losses are related to the loss of five water molecules (Calcd. 13.2, 13.5 %, respectively). The second stage occurs between 400 and 560 °C for both complexes **1** and **2** and corresponds to the release of the imip ligand. The corresponding weight losses are 60.7 and 60.1 % (Calcd. 62.9 and 64.1 % for **1** and **2**, respectively). After 560 °C, there is no further weight loss. The residues (23.9, 22.0 %) are identified as ZnO and CoO, respectively (Calcd. 23.1 and 22.4 %, respectively). As for complex **3**, the host framework was stable up to ca. 91 °C. The first weight loss of 6.4 % occurred between 91 and 160 °C, which is related to the removal of the three coordinated water ligands (Calcd. 7.3 %). The second stage came between 363 and 560 °C, corresponding to the release of the imip ligand; the observed weight loss was 60.7 % (Calcd. 58.0 %). No further weight loss was observed above 560 °C. The residue (obs. 32.9 %) is assigned to CdO (calcd. 34.7 %).

Conclusion

In summary, Zn, Co, and Cd coordination polymers were prepared under solvothermal conditions by using H_2imip as a ligand. The results show that H_2imip is a good candidate for the construction of coordination polymers with stable and intriguing structures. The coordination polymers of these different metals show different properties with respect to their thermal stability and fluorescence.

Supplementary material

Crystallographic data for the structures reported here have been deposited with CCDC [Deposition No. CCDC-1444712 (**1**), No. CCDC-1450294 (**2**), and No. CCDC-1450295 (**3**)]. These data can be obtained free of charge via http://www.ccdc.cam.ac.uk/conts/retrieving.htmlor from CCDC,12 Union Road, Cambridge CB2 1EZ, UK, E-mail: deposit@ccdc.cam.ac.uk.

Acknowledgments The authors thank the National Natural Science Foundation of China (21267003), P.R. China, the Natural Science Foundation of Guangxi (053020), P.R. China, and Guangxi University for Nationalities.

References

1. Batten SR, Champness NR, Chen XM, Javier GM, Kitagawa S, Öhrström L, O'Keeffe M, Suh MP, Reedijk J (2012) CrystEngComm 14:3001
2. Zhang CQ, Sun LB, Yan Y, Li JY, Song XW, Liu YL, Liang ZQ (2015) Dalton Trans 44:230
3. Wang K-X, Chen J-S (2011) Acc Chem Res 44:531
4. Hu JS, Shang YJ, Yao XQ, Qin L, Li YZ, Guo ZJ, Zheng HG, Xue ZL (2010) Cryst Grow Des 10:2676
5. Chandrasekhar V, Mohapatra C, Metre RK (2013) Cryst Growth Des 13:4607
6. Chen J, Li K, Chen L, Liu R, Huang X, Ye D (2014) Green Chem 16:2490
7. Zhu AX, Qiu ZZ, Yang LB, Fang XD, Chen SJ, Xu QQ, Li QX (2015) CrystEngComm 17:4787
8. Zhang CQ, Sun LB, Yan Y, Li JY, Song XW, Liu YL, Liang ZQ (2015) Dalton 44:230
9. Mihalcea I, Henry N, Bousquet T, Volkringer C, Loiseau T (2012) Cryst Growth Des 12:4641
10. Yang TH, Silva AR, Shi FN (2015) CrystEngComm 17:3852
11. Xie YB, Gan L, Sanudo EC, Zheng HY, Zhao JP, Zhao MJ, Wang B, Li JR (2015) CrystEngComm 17:4136
12. Yang F, Liu QK, Ma JP, Li YA, Wang KX, Dong YB (2015) CrystEngComm 17:4102
13. Murray LJ, Dinc AM, Long JR (2009) Chem Soc Rev 38:1294
14. Wu HH, Gong QH, Olson DH, Li J (2012) Chem Rev 112:836
15. Natarajan S, Mahata P (2009) Chem Soc Rev 38:2304
16. Fan RQ, Yang YL, Yin YB, Hasi W, Mu Y (2009) Inorg Chem 48:6034
17. Ling YJ, Song CL, Feng YL, Zhang MX, He YB (2015) CrystEngComm 17:6314
18. Zhang L, Zheng JD, Chen YT, Zheng SR, Fan J, Zhang WG (2015) CrystEngComm 17:5538
19. Ding B, Wang YY, Liu SX, Wu XX, Zhu ZZ, Huo JZ, Liu YY (2015) CrystEngComm 17:5396
20. Hu TP, Zhao YQ, Mei K, Lin SJ, Wang XP, Sun D (2015) CrystEngComm 17:5947
21. Zhang XQ, Gao YF, Liu HT, Liu ZL (2015) CrystEngComm 17:6037
22. Zhou YF, Lou BY, Yuan DQ, Xu YQ, Jiang FL, Hong MH (2005) Inorg Chim Acta 358:3057
23. Zhang XT, Fan LM, Fan WL, Li B, Zhao X (2015) CrystEngComm 17:6681
24. Zhang Z, Feng YF, Wei QY, Hu K, Chen ZL, Liang FP (2015) CrystEngComm 17:6724

25. Wang XL, Xu N, Zhao XZ, Zhang JW, Gong CH, Li TJ (2015) CrystEngComm 17:7038
26. Wang CC, Gao F, Guo XX, Jing HP, Wang P, Gao SJ (2016) Transit Met Chem 41:375–385
27. Liu SJ, Xie XR, Zheng TF, Bao J, Liao JS, Chen JL, Wen HR (2015) CrystEngComm 17:7270
28. Duan JG, Higuchi M, Zou CC, Jin WQ, Kitagawa S (2015) CrystEngComm 17:5609
29. Zhu SL, Ou S, Zhao M, Shen H, Wu CD (2015) Dalton 44:2038
30. Ye BH, Tong ML, Chen XM (2005) Coord Chem Rev 249:545
31. Sheldrick GM (2008) Acta Cryst 64:112
32. Mu YJ, Han G, Ji SY, Hou HW, Fan YT (2011) CrystEngComm 13:5943
33. Allendorf MD, Bauer CA, Bhakta RK, Houk RJT (2009) Chem Soc Rev 38:1330
34. Liu K, Ma BH, Guo XL, Ma DX, Meng LK, Zeng G, Yang F, Li GH, Shi Z, Feng SH (2015) CrystEngComm 17:5054